Check for updates

# Initial structural design approach for jacket-type substructure
# in 12 MW class offshore wind turbines considering soil stiffness

Joo-Shin Park[1] · Seon-Hyeok Kim[2] · Jung Kwan Seo†

**Abstract:** The wind power industry continues to grow, driven by environmental concerns such as achieving carbon neutrality, which has recently gained prominence. Creating wind farms poses several challenges due to limited land availability and insufficient wind resources. Consequently, offshore wind projects are garnering attention, particularly in domestic conditions. Notably, the Southwest Sea of Korea exhibits the highest offshore wind potential and has validated this potential through demonstrations. The primary geological characteristic of the Southwest Sea is a weak clay layer. To ensure the stable operation of generators, enhancing the precision of the substructure becomes imperative. This study presents an engineering procedure for developing a jacket-shaped wind turbine substructure, which was analyzed to assess the impact of soil properties on structural strength. In a previous study, wind turbine capacity targeted 5 MW. However, in alignment with the technological trend in the Southwest Sea offshore wind turbine market, this analysis model focuses on the 12 MW class. The structural response under varying soil conditions was verified using data from the North Sea, Mexico Bay, and Southwest Sea. The findings of this study not only contribute to designing structurally sound wind turbine substructures but also serve as essential reference data for engineers in related fields, providing insights into structural safety design and analytical verification processes.

**Keywords:** Offshore wind power, Substructure, Clay layer, Structural safety, Jacket type

## 1. Introduction

Countries worldwide are increasingly embracing new and renewable energy sources as a pivotal response to climate change, addressing the depletion of fossil fuels, mitigating greenhouse gas emissions, and generating employment opportunities. Consequently, the technology and market segments of related industries are experiencing rapid growth. One of the environmentally friendly methods for power generation is offshore wind power, harnessing wind energy from bodies of water such as oceans, lakes, fjords, and coastal regions. Wind power, which transforms mechanical energy generated by rotating blades according to aerodynamic principles into electrical energy through generators, boasts the highest efficiency among eco-friendly renewable energy sources.

Offshore wind power generation facilities can be broadly categorized into turbine structures, substructures, transmission facilities,



**Figure 1:** Fixed offshore wind turbine substructures

and turbine installation vessels. These installations can be further classified into fixed and floating types based on the method of securing the turbines to the seabed during installation.

**Figure 1** illustrates various types of fixed offshore wind turbine substructures, offering a comprehensive overview of these structures [1].

In general, offshore wind turbines (OWT) are installed at

† Corresponding Author (ORCID: http://orcid.org/0000-0002-3721-2432): Professor, Department of Naval Architecture and Ocean Engineering/The Korea Ship and Offshore Research Institute, Pusan National University, 2, Busandaehak-ro, Geumjeong-gu, Busan 46241, Korea, E-mail: seojk@pusan.ac.kr, Tel: +82-51-510-2415

1 Principal Engineer, Ship and Offshore Research Institutes, Samsung Heavy Industries, E-mail: scv7076@nate.com, Tel: +82-55-630-9613

2 M. S. Candidate, Department of Naval Architecture & Ocean Engineering, Pusan National University, E-mail: seonhyeok@pusan.ac.kr, Tel: +82-51-510-2750

**Copyright ⓒ The Korean Society of Marine Engineering**

Joo-Shin Park ・ Seon-Hyeok Kim ・ Jung Kwan Seo

depths of 70 m or less, supported by fixed substructures on the seabed. The types of substructures, including mono-piles, triangular buckets, and jacket structures (refer to **Figure 2**), are deployed at water depths of approximately 25 m, 50 m, and 70 m, respectively. With the growing capacity of OWT, jacket-type substructures have emerged as highly competitive options due to their usability and versatility.

Notably, in many areas where offshore wind farms are anticipated, such as the southwest coast of Korea (Gunsan, Shinan, and Yeonggwang), the prevailing soft clay soil conditions present a challenge due to their low stiffness. Consequently, a thorough investigation into the design applicability of jacket-type substructures for OWT is essential to account for these unique ground conditions.
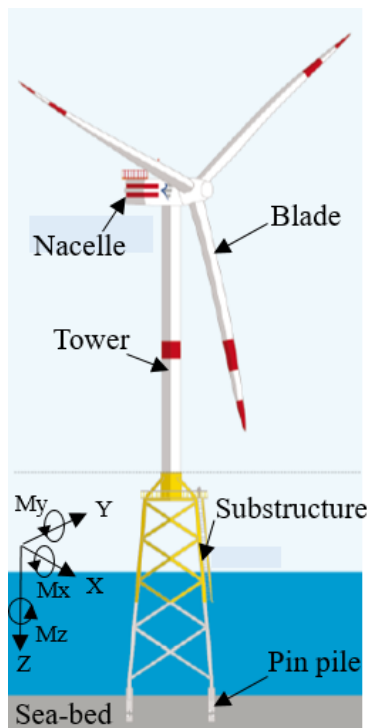


**Figure 2:** Illustration of an offshore wind turbine on jacket-type substructure

Prior research in this domain has yielded several insights. Chew *et al.* **[2]** explored both conventional four-legged and newly developed three-legged bottom-fixed jacket substructures for offshore wind applications. Their study encompassed fatigue (FLS) and ultimate limit state (ULS) analyses, which indicated the feasibility of the three-legged concept as a potentially cost-efficient alternative to the four-legged design, offering a 17% reduction in structural mass and a 25% reduction in the number of welded joints. Additionally, they recommended finer incident

angle resolution (a gap of 15° or less) for sensitivity analysis of dynamic performance.

Kim *et al.* **[3]** delved into the effects of substructures on the ultimate loads of OWT, using the National Renewable Energy Laboratory (NREL) 5-MW generic model. They compared the dynamic characteristics of ultimate loads between monopile and jacket-type models, determining forces and moments on the blade, tower, hub, and yaw-bearing sections. However, their model's applicability is constrained due to its reliance on the NREL standard model.

Yi *et al.* **[4]** investigated monopile, tripod, and jacket-supported OWT concerning pile-soil interaction effects. Their research revealed that the stiffness of soil springs decreases with increasing equivalent loading amplitude, leading to a slight reduction in natural frequency, which may be negligible for practical purposes in the case of tripod and jacket-supported turbines. Notably, the monopile type exhibited more significant natural frequency variation with changing equivalent load amplitudes.

Hafele *et al.* **[5]** proposed decision guidance for the initial phase of wind farm planning and provided a numerical example using an NREL 5 MW turbine under FINO3 environmental conditions. They employed two effective optimization methods to estimate characteristic design variables of a jacket substructure. The numerical results indicated that three-legged jackets may be preferable to four-legged designs within certain boundaries, and mass-dependent cost functions could be enhanced by considering the number of jacket legs, leading to more reliable outcomes.

Lee *et al.* **[6]** conducted a comparative analysis of international and national design standards for jacket substructures applicable to wind farms on the southwest coast of Korea. They compared the design criteria with those of the Korean Register (KR) and Det Norske Veritas (DNV), finding that KR's criteria yielded conservative evaluation results. This divergence primarily stemmed from the differences in load factor and resistance factor safety factors used in safety evaluation, with discrepancies of up to 5%. Their comparative review confirmed the reasonableness of KR's evaluation procedure and safety standards for the design of offshore wind power support structures constructed in Korea.

Cao *et al.* **[7]** explored differences in dynamic responses between an OWT model employing the traditional p-y method and a new model. Numerical analysis revealed that the traditional p-y method tended to overestimate top displacements of the OWT under stochastic wind and wave loads. Furthermore, the study investigated the effects of wind-wave combinations, wind-wave

misalignment angles, and operational conditions on structural responses. The combination of 90° wind-wave angles and operating conditions emerged as the most unfavorable scenario.

Prior studies primarily focused on calculating dynamic responses and developing lightweight models to optimize substructure configurations, with most of these studies centered around 5 MW wind turbines, differing from the more recent 12 MW wind turbines. Notably, investigations into environments characterized by soft clay layers were insufficient, highlighting a gap in research on simplifying soil effects with nonlinearity from an engineering perspective. Thus, this study aims to propose and verify a procedure for a jacket substructure that ensures installation structural safety while accounting for the soil-bearing capacity characteristics of soft clay seabeds.

## 2. Design Condition

### 2.1 Basic Design of Substructures

The fundamental concept and procedures for the basic and detailed design of offshore wind turbine substructures are illustrated in **Figure 3 [8]**. During the basic design phase, design factors and criteria are established, and an appropriate substructure method **[9]** is selected based on the soil characteristics of the seabed installation conditions. In the subsequent detailed design stage, detailed structural components are analyzed under environmental and operational conditions to ensure they meet the necessary structural safety requirements. The design of the pin piles used to secure the foundation is also scrutinized, taking into account soil effectiveness.

Before proceeding to the detailed design, reaction force data from operational conditions are utilized to assess the substructure's structural integrity. Prior to finalizing the manufacturing drawings, analysis results for structural members are incorporated, and if any members fail to meet safety requirements, a process of redesign and reinforcement is undertaken.

Following the basic design procedure (as depicted in **Figure 3**), the specific wind farm and installation seabed site in the South-western Sea of Korea are selected. The loads and moments acting on the primary structural members are computed based on the substructure's basic design. Additionally, a design methodology considering the characteristics of the detailed soil-bearing capacity is developed using information specific to the chosen seabed.
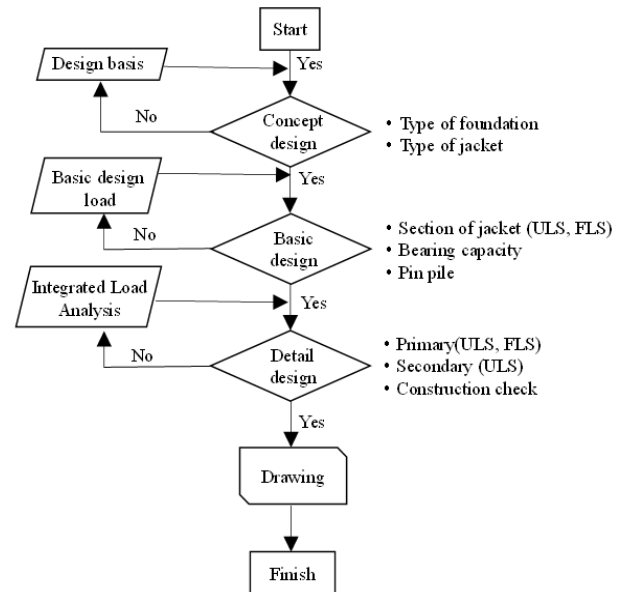


**Figure 3:** Design flow chart and check items

To begin, the self-weight component affecting the jacketed offshore wind turbine structure is divided into the upper structure's weight (nacelle, blade, tower) and the lower structure's weight (see **Figure 2**). Environmental loads are designed by assessing the structure's safety, taking into account dynamic load components associated with a 50-year return period, including wind, waves, wind-induced generator vibration, and earthquakes.

Wave loads are determined using the Morrison formula, which incorporates a stream function describing particle trajectories in steady wave flows within a sea area. The wave load impacting a structure primarily depends on wave height, which exhibits period-dependent effects. However, establishing a direct relationship between wave height and wave direction proves challenging due to location-specific variations. Consequently, this study employs a wave height of 10.3 m, a wave period of 13.2 s, and a wind speed of 50 m per second for the 50-year return period design wave, calculated through long-term wave analysis. Moreover, meteorological conditions during typhoons are considered.

Earthquake loads are omitted from consideration due to the pin pile's connection to the rock layer, in line with the characteristics of the jacket-type substructure.

Furthermore, the wind load affecting the upper structure induces changes in sea level amplitude as wind speed increases, leading to heightened turbulence intensity. The design accounts for the effect of sea-surface roughness **[10]**, factoring in changes in wind speed.

Joo-Shin Park · Seon-Hyeok Kim · Jung Kwan Seo

The structural shape chosen for the substructure is an inclined jacket-type, minimizing displacement and stress at the substructure and connection points during wind turbine installation, and offering optimal dynamic response to loads. This substructure, featuring four pin piles, provides excellent stability and a wide fixation area compared to vertical alternatives.

These advantages facilitate a design that avoids resonance with the wind turbine, while minimizing the surface area exposed to environmental forces such as currents, waves, and wind.

Detailed dimensions and structural members based on the sub-structure FE model are outlined in **Figure 4** and **Table 1**. Structural simulations were conducted using the SACS computer structural analysis program **[11]**. All structural steel employed in the construction is high-tensile steel (EH36) with a yield stress of 355 MPa. In the leg and brace connection joints (Cans), localized thickness increases are applied due to in-plane stress concentration phenomena, with modeling results depicted in **Figure 4** using member outer diameter information.

Loading conditions **[12]** are categorized into force and moment components, as outlined in **Table 2** and **Table 3**, respectively.

**Table 1:** Member dimensions according to member type

| Grade | Type | Outer diameter (O.D) (mm) | Thickness(mm) |
|---|---|---|---|
| S355 | Leg can | 2,170 | 36 |
| | Leg | 2,140 | 22 |
| | Brace can | 1,070 | 36 |
| | Brace | 1,050 | 22 |
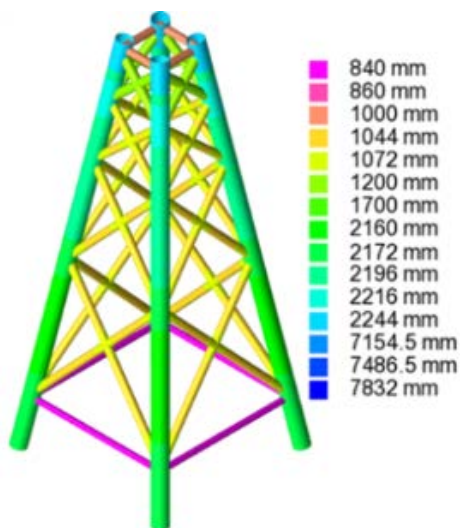


**Figure 4:** FE model and diameter of leg and brace members

**Table 2:** Summary of the forces

| No. | L.C. | Force(kN) | | |
|---|---|---|---|---|
| | | Fx | Fy | Fz |
| 1 | TB01 | - | - | -16.471 |
| 2 | TB02 | - | - | -16.471 |
| 3 | TB03 | - | - | -16.471 |
| 4 | TB04 | - | - | -16.471 |
| 5 | TB05 | - | - | -16.471 |
| 6 | TB06 | 3,600 | 3,600 | -16.471 |
| 7 | TB07 | - | - | -16.471 |
| 8 | TB08 | 3,400 | - | -16.471 |
| 9 | TB09 | - | 3,400 | -16.471 |
| 10 | TB10 | 3,900 | 3,900 | -16.471 |
| 11 | TB11 | 3,700 | 3,700 | -16.471 |
| 12 | TB12 | - | - | -16.471 |

Notes: L.C.: Loading Condition Fx, Fy and Fz determined in each directional force

**Table 3:** Summary of the moments

| No. | L.C. | Moment(kN·m) | | |
|---|---|---|---|---|
| | | Mx | My | Mz |
| 1 | TB01 | 370,000 | - | - |
| 2 | TB02 | - | 370,000 | - |
| 3 | TB03 | 333,000 | - | - |
| 4 | TB04 | - | 333,000 | - |
| 5 | TB05 | 370,000 | 370,000 | - |
| 6 | TB06 | 370,000 | 370,000 | - |
| 7 | TB07 | - | - | 45,300 |
| 8 | TB08 | - | - | - |
| 9 | TB09 | - | - | - |
| 10 | TB10 | 310,000 | 310,000 | - |
| 11 | TB11 | 357,000 | 357,000 | - |
| 12 | TB12 | - | - | 43,800 |

Notes: L.C.: Loading Condition Mx, My and Mz determined directional rotating moment

## 2.2 Soil and Corrosion Conditions

To assess the seabed's bearing capacity at the designated wind farm location in the South-western Sea of Korea, we assumed that the ground characteristics consisted of clay layers extending approximately 17 m from the seabed, transitioning to rocks beyond that depth.

In particular, we examined the limit state conditions for the clay layer, utilizing clay layer stiffness data from the North Sea and Gulf of Mexico (GoM), along with penetration test data from an offshore wind farm in the Southwestern Sea of Korea **[13]**-**[14]**. An FE model was applied to simulate the length of the pin

pile penetrating the substructure, as depicted in **Figure 5**. Typically, a pin pile is installed in the soil depth direction, comprising vertical stiffness ($K_z$), horizontal stiffness ($K_x$), and rotational stiffness ($K_\theta$), as illustrated in **Figure 6**. The detailed soil stiffness values applied are presented in **Table 4**. Notably, it was observed that the coefficient of soil stiffness in the North Sea exceeded that in the Southwest Sea for the same clay layer by more than tenfold. This discrepancy can be attributed to the distinctive soil characteristics found in the target seabed.
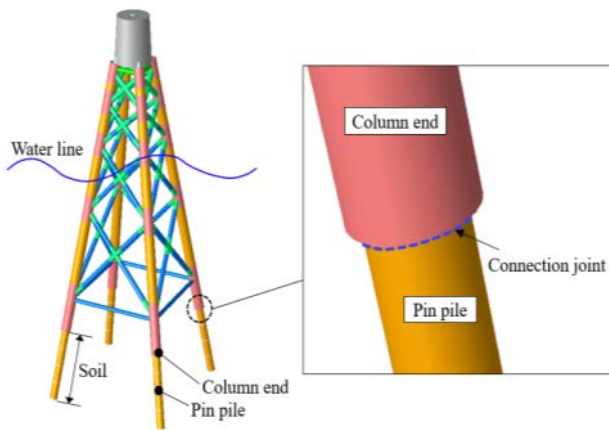


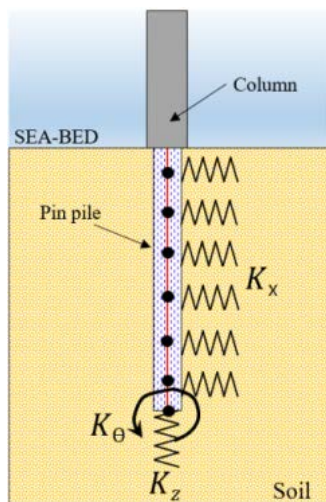**Figure 5:** Substructure model with pin pile



**Figure 6:** Soil application around the pin pile

**Table 4:** Summary of soil stiffness at installation sites

| Location | Soil stiffness | | |
| --- | --- | --- | --- |
| | $K_z$ (MN/m) | $K_x$ (MN/m) | $K_\theta$ (MN·m/deg) |
| Southwestern sea of Korea | 418 | 308 | 375 |
| North sea | 5,143 | 3,790 | 4,616 |
| GoM | 579 | 426 | 519 |

To account for the corrosion impact of seawater on jacket structural members, we categorized them based on the magnitude of wave load fluctuations **[15]**. As depicted in **Figure 7**, we assumed that the inner and outer surfaces of the pipes would equally degrade by 0.1 mm per year from the seabed to a depth of 34.2 m, resulting in a total thickness loss of 2.0 mm. From the water surface to the seabed at a depth of 9.4 m, the inner surface of the pipe was assumed to lose 0.2 mm, while the outer surface would lose 0.4 mm per year. Additionally, we considered the area above the water surface, unaffected by seawater, which would experience a reduced corrosion rate of 2 mm over a span of 20 years.
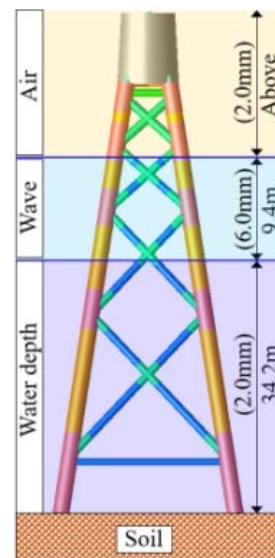


**Figure 7:** Application of corrosion based on DNV requirement

### 2.3 Environmental Loads and Load Factors

The maximum wave height was determined to be 19.3 m, based on the 50-year return period wave height for the wind turbine and substructure's design wave conditions. Consequently, in the case of the substructure, we accounted for a 50 mm increase in thickness due to the accumulation of marine sediments below sea level. Additionally, for a conservative structural strength design, we configured the directions of local and environmental loads generated during generator operation to be the same.

**Table 5** provides details of five load conditions derived from the return period of the ULS design. It was possible to assess all five combinations and formulate a design that met the criteria mentioned above. Based on the limit states during the load combinations, three ULSs are categorized as presented in **Table 6 (a)** and **(b)** correspond to conditions primarily influenced by

Joo-Shin Park ・ Seon-Hyeok Kim ・ Jung Kwan Seo

environmental loads, while **Table 6 (c)** represents an abnormal wind load situation condition.

**Table 5:** Components of the environmental loads and return period

| L.S | L.C | Wind | Wave | Current | Ice |
|-----|-----|------|------|---------|-----|
| ULS | 1 | 50-yr | 5-yr | 5-yr | - |
| | 2 | 5-yr | 50-yr | 5-yr | - |
| | 3 | 5-yr | 5-yr | 50-yr | - |
| | 4 | 5-yr | - | 5-yr | 50-yr |
| | 5 | 50-yr | - | 5-yr | 50-yr |

**Table 6:** Basic load factor in ULS

| SET | Limit states | Load categories | | | |
|-----|--------------|------|------|------|------|
| | | G | Q | E | D |
| (a) | ULS | 1.25 | 1.25 | 1.00 | 1.00 |
| (b) | ULS | 1.00 | 1.00 | 1.35 | 1.00 |
| (c) | ULS for abnormal wind load cases | 1.00 | 1.00 | 1.10 | 1.00 |

Notes: G is permanent loads such as tower weight, jacket pile weight, Q is variable functional loads according to boat impact, E is environmental loads such as extreme wind and wave loads, tidal and marine growth effect, and D is deformation loads such as temperature, built-in deformation, creep load
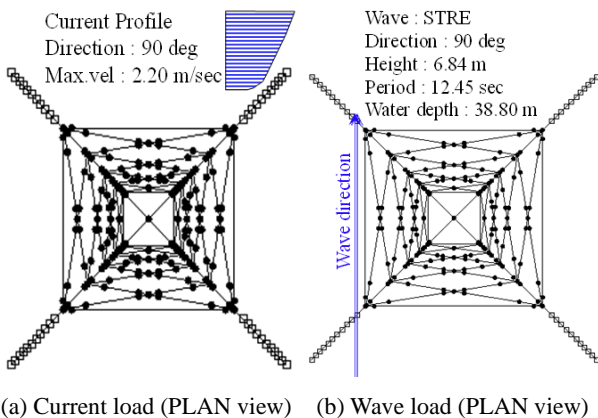


(a) Current load (PLAN view)　(b) Wave load (PLAN view)

**Figure 8:** Current load wave load at the heading angle of 90 degrees

**Figure 8** illustrates the outcomes of applying current and wave loads to the analysis model at an incident angle of 90°. In the case of wave loads, details such as wave theory, height, and period are provided, with the incident angle's direction indicated by an arrow. Furthermore, the current load was considered, taking into account the velocity gradient from the seabed to the surface, with a maximum speed of 2.2 m/s explained.

## 3. FE based Structural Evaluation

### 3.1 FE Modeling and Loads

We employed the SACS code, a commercial offshore finite element analysis tool, to model and analyze the structural strength. **Figure 9** illustrates the jacket's lower structure, including the four pillars used in our study. The modeling, depicting the structure connecting the wind turbine installed on the upper part and the lower structure, is presented on the left side of **Figure 9**. The right side of the figure shows the state without a transition piece. In this study, we utilized the reaction force generated during wind turbine operation for load combinations, evaluating the lower structure's strength using the modeling displayed on the left side of **Figure 9**.
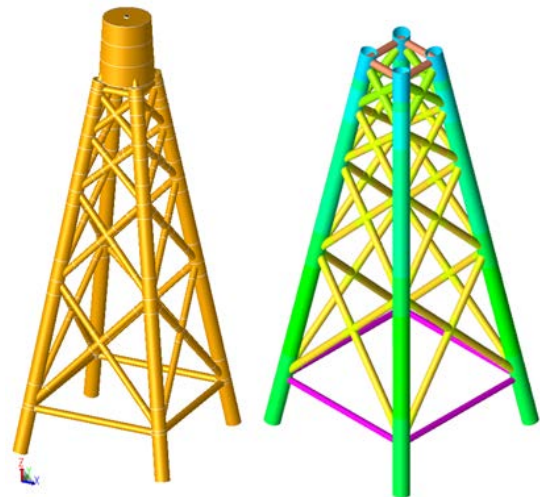


**Figure 9:** Analysis model of the substructure (left: with transition piece, right: without transition piece)

**Table 7:** Material properties of the substructure

| Properties | Specification |
|------------|---------------|
| Elastic Modulus | 205,800MPa |
| Poisson's ratio | 0.3 |
| Density | 78.5kN/m3 |
| Yield strength (structure) | 355MPa |
| Yield strength (pin pile) | 235MPa |
| Tensile ultimate strength | 420MPa |
| Tensile Strain at break | 15% |

The ends of the four pillars in the substructure incorporate pin piles that penetrate the interior. These pillars are comprised of 232 joints and 291 members, with 1,844 member sections used.

We classified single loads into 93 types and derived 193 types of load combinations. The structural members' material properties were considered to be high-tensile steel and mild steel, with detailed information provided in **Table 7**.

### 3.2 Results of Structural Strength

In this study, we applied EUROCODE **[16]** as the criterion for structural safety evaluation. While EUROCODE is not exclusive to offshore wind turbine substructure design, it enjoys widespread adoption in evaluating the safety of jacket-type structures due to its high reliability.

Among the ultimate limit state design conditions (ULS-(a)), we analyzed the highest unity check (UC) results, specifically 0.995 for the main column member and 0.610 for the brace. These results satisfy the structural strength criteria, with values less than the acceptance criterion of 1.0. The member size and stress result information are summarized in **Table 8**.

**Table 8:** Detailed results of maximum stress at the column

| Dimension and stress | Value |
|---|---|
| O.D(outer diameter) | 2,148mm |
| Wall thickness | 28mm |
| Material factor | 1.15 |
| Fa(axial stress) - maximum | -254.73MPa |
| Fb(bending stress) - maximum | 53.40MPa |
| Fa(axial stress) - allowable | 304.92MPa |
| Fb(bending stress) - allowable | 335.05MPa |

### 3.3 Effect of Fixation

**Figure 10** presents a comparison of the maximum combined stress under the pin-pile condition (simply supported condition) and the assumption of fixed ends for the substructure. Similar stress ratios were observed when applying ground-fixing effects of the pin pile and arbitrary boundary conditions. This can be attributed to the substantial confinement effect resulting from the stiffness of the surrounding soil, given the sufficiently deep penetration length of the pin pile.

To assess the substructures' structural strength based on boundary conditions, **Figure 10** and **Table 9** compare the analysis results when fixed conditions were applied, incorporating the stiffness of three clay layers. The maximum U.C. of the vertical column yielded similar results to those when the pin pile was applied. The highest values were observed in the North Sea. Without the pin pile, the evaluation was 1% smaller, based on the maximum U.C.
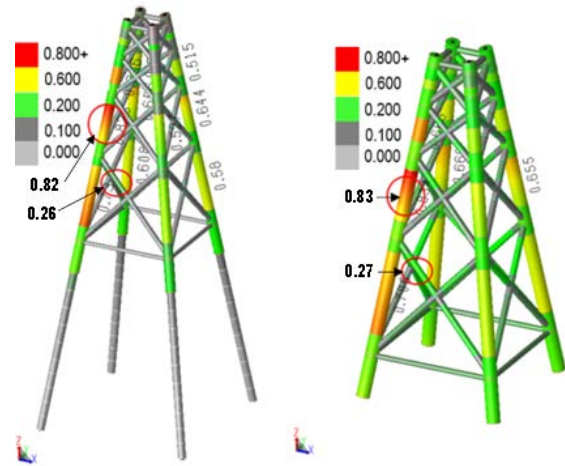


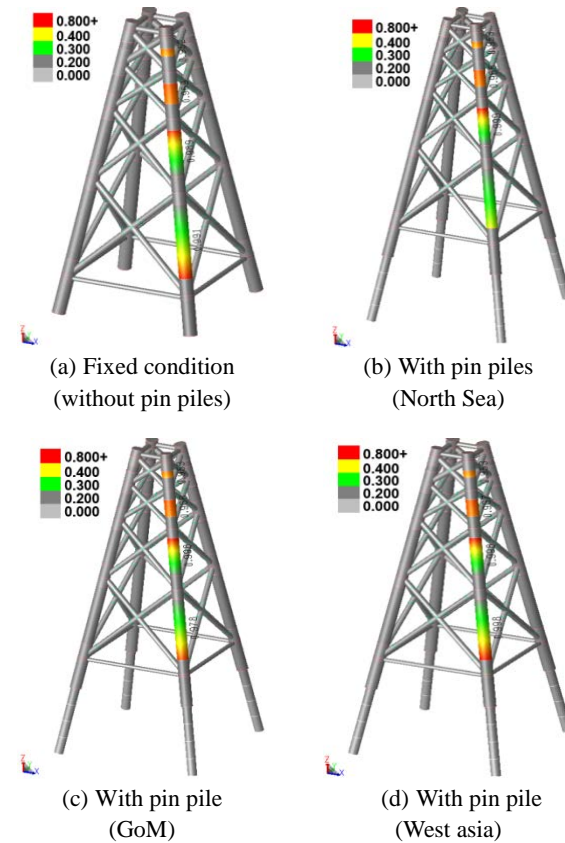**Figure 10:** Combined unity ratio according to end fixity



(a) Fixed condition
(without pin piles)

(b) With pin piles
(North Sea)

(c) With pin pile
(GoM)

(d) With pin pile
(West asia)

**Figure 11:** Results of maximum combined UC according to soil stiffness

**Table 9:** Maximum U.C results according to boundary conditions

| Boundary condition | Maximum U.C | Allowable U.C |
|---|---|---|
| Fixed condition | 0.991 | |
| Soil-North sea | 0.999 | 1.000 |
| Soil-GoM | 0.998 | |
| Soil-West asia | 0.998 | |

Joo-Shin Park · Seon-Hyeok Kim · Jung Kwan Seo

Considering these results, we acknowledge the challenge of obtaining geological data during the initial design and the considerable experience and time required for nonlinear soil analysis. Consequently, in the initial weight review, we determined that substituting the effect of the pin pile with a fixed condition, based on the findings of this study, is sufficient to establish the steel's order.

## 4. Conclusion

In this study, we proposed a design factor to determine the strength and bearing capacity period for the jacket-type substructure of a substantial 12 MW offshore wind turbine. We confined our analysis to the clay layer and incorporated the fixation effect around the pin pile by referencing geological survey literature from the North Sea, GoM, and Southwest Sea. The FE code (SACS) was utilized to ascertain the substructures that met EUROCODE design criteria. Our study's conclusions are summarized as follows:

1. Consideration of soil stiffness is essential to account for the impact of pin-pile support on the substructures. Soil stiffness values, encompassing vertical, horizontal, and rotational aspects, should be applied in the height direction.

2. In our analysis using the pin pile, differences in geological stiffness yielded very marginal variations, with the largest discrepancy observed in the North Sea condition.

3. Applying a fixed support condition to the substructure's end without a pin pile allows for quicker determination of structural member design compared to current industry practices.

4. The maximum unity U.C. occurred in the vertical column, with primary load components being compressive and bending stresses. These findings were substantiated by four inclined pillar members.

For future research, it is advisable to explore alterations in the inclination angle and arrangement of the column members comprising the jacket substructure. Additionally, investigating load distribution models that minimize weight and developing new joints to enhance the welding workability of circular pipe connections would be beneficial avenues of study.

## Acknowledgement

## Author Contributions

Conceptualization, J. S. Park; Methodology, J. S. Park; Formal Analysis, J. S. Park; Writing-Original Draft Preparation, J. S. Park and S. H. Kim; Writing-Review & Editing, J. K. Seo; Visualization, J. S. Park and S. H. Kim; Supervision, J. K. Seo; Funding Acquisition, J. K. Seo.

## References

[1] Tethys, Fixed Offshore Wind, https://tethys.pnnl.gov, Accessed April 14, 2023.

[2] K. H. Chew, E. Y. K. Ng, and K. Tai, M. Muskulus, and D. Zwick, "Offshore wind turbine jacket substructure: A comparison study between four-legged and three-legged designs," Journal of Ocean and Wind Energy, vol. 1, no. 2, pp. 74-81, 2014.

[3] B. S. Kim, J. W. Jin, O. Bitkina, and K. W. Kang, "Ultimate load characteristics of NREL 5MW offshore wind turbines with different substructures," International Journal of Energy Research, vol. 40, no. 5, pp. 639-650, 2016.

[4] J. H. Yi, S. B. Kim, T. H. Han, G. L. Yoon, and L. V. Anderson, "Influence of pile-soil-interaction on natural frequency of bottom-fixed offshore wind turbines considering material uncertainties," The 2015 World Congress on Advances in Civil, Environmental and Materials Research (ACEM15), pp. 25-29, 2015.

[5] J. Hafele, C. G. Gebhardt, and R. Rolfes, "A comparison study on jacket substructures for offshore wind turbines based on optimization," Wind Energy Science, vol. 4, no. 1, pp. 23-40, 2019.

[6] K. H. Lee, S. K. Park, G. H. Kim, and T. G. Hwang, "Basic design of a flange connected transition piece between offshore wind turbine and monopile foundation," Transaction of the Korean Hydrogen and New Energy Society, vol. 31, no. 1, pp. 160-168, 2020 (in Korean).

[7] G. Cao, Z. Chen, C. Wang, and X. Ding, "Dynamic response of offshore wind turbine considering soil nonlinearity and wind-wave load combinations," Ocean Engineering, vol. 217, pp. 50-58, 2020.

[8] K. C. Seo, J. S. Choi, and J. S. Park, "Development of foundation structure for 8mw offshore wind turbine on soft clay layer," Journal of the Korean Society of Marine Environment & Safety, vol. 27, no. 2, pp. 394-401, 2021.

[9] J. S. Park and J. K. Seo, "Development of a unified formula for evaluating the safe working loads of ship block support

structures," Journal of Advanced Marine Engineering and Technology, vol. 46, no. 3, pp. 107-114, 2022.

[10] IEC 61400-3-1, Wind energy generation systems-Part 3-1: Design requirements for fixed offshore wind turbines. International Electrotechnical Commission, 2019.

[11] SACS User's manual, Introduction of linear and nonlinear analysis and it's application of shell modelling. Bently systems, 2018.

[12] GE Renewable Energy, HALIADE-X Technical Building Specification, Document RDS-PP Code, pp. 1-16, 2020.

[13] IADC, The calibration of SNAME spudcan fixity equations with field data. Report No. L19073/NDE/MJRH, 2015.

[14] Soil measurement report, Optimized leg design and development of jack-up system for wind turbine installation vessel(WTIV), Project No.20123010020090, pp. 3-7; 23-69, 2013.

[15] DNV, Fixed Offshore Wind Structure Design, Detailed Design-Modeling, pp. 7-15, 2022.

[16] BS EN 1993-1-1, Eurocode 3: Design of steel structures.